Cylindrical lateral depth-sensing indentation of anisotropic elastic tissues

Argatov, Ivan; Mishuris, Gennady

Published in:
Journal of Adhesion

DOI:
10.1080/00218464.2017.1309524

Publication date:
2017

Citation for published version (APA):
Argatov, I., & Mishuris, G. (2017). Cylindrical lateral depth-sensing indentation of anisotropic elastic tissues: Effects of adhesion and incompressibility. *Journal of Adhesion*, *94*(8), 583-596. https://doi.org/10.1080/00218464.2017.1309524

ORIGINAL ARTICLE

Cylindrical lateral depth-sensing indentation of anisotropic elastic tissues: Effects of adhesion and incompressibility

I. Argatov[a] and G. Mishuris[b]

[a]Institut für Mechanik, Technische Universität Berlin, 10623 Berlin, Germany; [b]Department of Mathematics, Institute of Mathematics, Physics and Computer Science, Aberystwyth University, Ceredigion SY23 3BZ, Wales, UK

ARTICLE HISTORY
Compiled March 18, 2017

Abstract
A two-dimensional frictionless adhesive contact problem for a parabolic indenter pressed against an orthotropic elastic layer resting on a smooth rigid substrate is studied in the framework of the Johnson–Kendall–Roberts (JKR) theory. In the case of a relatively small contact zone with respect to the layer thickness, the fourth-order asymptotic solution (up to terms of order $O(\varepsilon^8)$) is obtained, and the pull-off force is expanded in terms of the non-dimensional measure of the work of adhesion. In particular, a pinch/compression method for soft tissue is considered, and the testing methodology is suggested based on a least squares best fit of the first-order asymptotic model to the depth-sensing indentation data for recovering two of the three independent elastic moduli which characterize an incompressible transversely isotropic material. The case of a weakly compressible material, which is important for biological tissues, is also discussed. The developed asymptotic model can be effectively used for small values of a certain dimensionless parameter, which is proportional to the work of adhesion and the indenter radius squared, on the one side, and inversely proportional to the effective elastic modulus and the elastic layer thickness cubed, on the other.

KEYWORDS
Analytical models; non-destructive testing; adhesion/non-stick; indentation testing; transversely isotropic; incompressible

1. Introduction

Indentation testing both *in vivo* and *in vitro* becomes more and more popular in application to biological tissues [1], since the tissue stiffness is often sensitive to pathological structural alterations [2,3]. Therefore, there is a need for the development of reliable analytical models for the interpretation of the continuous stiffness measurements [4], and in particular for depth-sensing indentation measurements of the mechanical properties of *in vivo* human skin including its anisotropic characteristics [5].

It is well known that many biological tissues are characterized by anisotropy [6] and adhesion [7], and the case of transverse isotropy plays an important role for describing their elastic properties [8]. In particular, the skin adhesive behaviour is important in the dermatological and cosmetic fields and can be effectively assessed by indentation testing [9].

In recent years, a variety of indentation techniques have been introduced, which can be classified by the indenter type (e.g., flat-ended cylindrical, spherical, pyramidal, etc.). Specifically with application to *in vivo* measurement of properties of human tissue, Harrison et al. [10] developed a localised indentation method based on the concept of pinching a section of tissue using two pinch rigid cylinders of finite length. In a first approximation, such a pinch test is modeled

CONTACT I. Argatov. Email: ivan.argatov@gmail.com

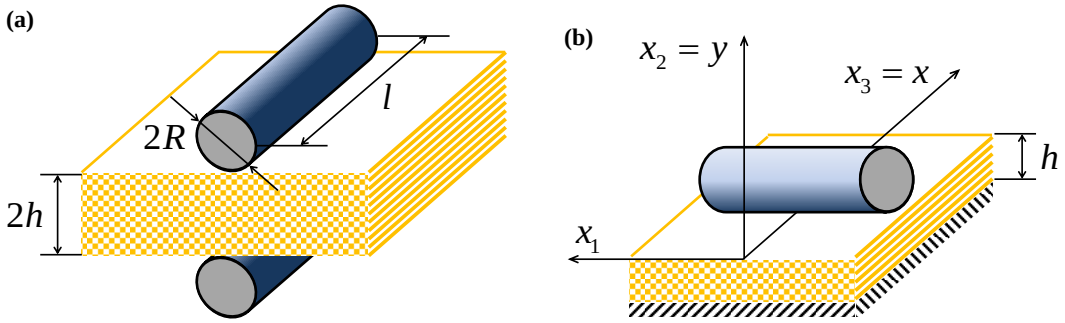

Figure 1. Schematic of the pinch/compression test: (a) An elastic layer of half thickness h compressed by two rigid cylinders of the same radius R; (b) An elastic layer of thickness h deposited onto a frictionless rigid substrate and indented by a rigid cylinder of radius R.

as a symmetric compression of an elastic layer (see Fig. 1b), which in turn is equivalent to the contact problem for an elastic layer with the frictionless bilateral boundary conditions $u_2 = 0$ and $\sigma_{12} = \sigma_{32} = 0$ at the interface $x_2 = -h$.

Recently, the so-called cylindrical lateral indentation test, which utilizes lateral contact of a cylindrical indenter (see Fig. 1b), was developed under the assumption that both Poisson's ratios of the tested transversely isotropic elastic material are known. Such a test can be approximately modeled [11] in the framework of the two-dimensional contact model for an orthotropic elastic strip, which was was studied previously by Aleksandrov et al. [12,13]. We note that in our asymptotic model it is assumed that the film thickness h and the indenter radius, R, should be small compared to the cylinder indenter length, l, as well as the contact zone size, a, should be small compared to the elastic film thickness h.

However, although it is usual to assume in the indentation testing of an isotropic material that its Poisson's ratio is known in advance [14], this assumption in the case of material anisotropy requires a careful consideration, especially for almost incompressible materials. On the other hand, in the case of incompressible transversely isotropic material, the previously developed model [11] needs to be further refined. In the present paper, the two-dimensional frictionless adhesive contact problem for a parabolic indenter pressed against an orthotropic elastic layer resting on a smooth rigid substrate is studied in the framework of the Johnson–Kendall–Roberts (JKR) theory [15]. The recent results related to extension of the JKR theory, and their relations to nanoindentation have been discussed in an extensive review by Borodich [16]. In particular, the JKR-type adhesive contact problems for transversely isotropic elastic solids were studied in a number of papers [17–19].

The rest of the paper is organized as follows. In Section 2, the JKR adhesive contact problem is formulated for a transversely isotropic elastic layer deposited onto a rigid substrate. The fourth-order asymptotic solution is written out in explicit form in Section 3. The corresponding asymptotic approximation for the pull-off force is presented in Section 4. In Section 5, the developed analytical solution is compared with the numerical solution obtained recently by Dalmeya et al. [20] in the isotropic case. The case of non-adhesive contact for an incompressible material is considered in Section 6, where the material identification procedure for the cylindrical lateral indentation test is outlined. Finally, in Sections 7 and Section 8, we present a discussion of the results obtained and formulate our conclusions, respectively.

2. Cylindrical lateral indentation of an adhesive elastic layer

In what follows, we assume that the tissue thickness, h, is small compared to the cylinder indenter length, l, so that the stress-strain state in the pinch zone can be modeled in the framework of plane elasticity (see Fig. 1b). Therefore, the indentation test under consideration can be reformulated in terms of the two-dimensional contact problem for an orthotropic elastic layer deposited on a rigid substrate, which, in turn, can be reduced to the following integral

equation [12]:

$$\frac{2}{\pi E^*}\int\limits_{-a}^{a} q(x')\int\limits_{0}^{\infty}\frac{L(u)}{u}\cos\Big(u\frac{x'-x}{h}\Big)\,du dx' = w - \frac{x^2}{2R}, \quad |x| \le a. \tag{1}$$

Here, $q(x)$ is the contact pressure, w is the indenter displacement, a is the half-width of the contact area, which is a priori unknown, R is the radius of the cylindrical indenter, E^* is the effective elastic modulus, $L(u)$ is the kernel function, which depends both on the orientation of the anisotropy planes and on the boundary conditions at the layer/substrate interface.

Integrating the contact pressure across the contact zone, we introduce the contact force per unit length

$$\mathcal{P} = \int\limits_{-a}^{a} q(x)\,dx,$$

while an additional integration along the contact zone yields the contact force

$$P = \mathcal{P}l, \tag{2}$$

where l is the cylinder indenter length.

In view of applications to soft tissues, we employ the JKR (Johnson–Kendall–Roberts) theory [15] of adhesive contact, which take into account only the surface forces inside the contact zone. The JKR theory was originally developed for a circular contact area and afterwards generalized by Maugis [21], who using the Griffith energy balance approach, introduced the following condition:

$$\frac{K_{\rm I}^2}{2E^*} = \Delta\gamma. \tag{3}$$

Here, $\Delta\gamma$ denotes the work of adhesion, $K_{\rm I}$ is the stress intensity factor (SIF), which at the point $x = \pm a$ is defined by the limit formula

$$K_{\rm I}^{\pm} = -\lim_{x\to\pm a}\sqrt{2\pi(a\mp x)}q(x). \tag{4}$$

We note that Johnson et al. [15] derived the adhesive contact model using energy balance solution, and later it was generalized by Maugis [21] in the framework of LEFM (Linear Elastic Fracture Mechanics), where Eq. (3) plays a fundamental role.

Thus, Eqs. (1), (2), and (3) constitute the JKR adhesive contact problem for an elastic layer. Note that in the non-adhesive unilateral contact problem, the contact size parameter a should be determined from the condition that the contact pressure $q(x)$ vanishes at the end points $x = \pm a$ being positive inside the contact zone for $x \in (-a, a)$, so that $K_{\rm I}^{\pm} = 0$.

3. Contact pressure in the pinch zone and the force-displacement relation

Under the assumption that the width of the contact zone is small compared to the tissue thickness, the following asymptotic solution was obtained [11]:

$$\begin{aligned} q(x) \;\simeq\; & \frac{1}{\pi a\sqrt{1-\xi^2}}\Bigg\{\mathcal{P}+\frac{\pi E^* a^2}{4R}\Big[1-2\xi^2+\varepsilon^4\frac{3d_2}{2}(1-2\xi^2)+\varepsilon^6\frac{15d_3}{8}(3-8\xi^4)\Big] \\ & -\mathcal{P}\Bigg(\varepsilon^2 d_1(1-2\xi^2)+\varepsilon^4\frac{d_2}{2}(7-8\xi^2-8\xi^4) \\ & +\varepsilon^6\Big[\frac{3d_1d_2}{2}(1-2\xi^2)+\frac{3d_3}{4}(13+6\xi^2-36\xi^4-8\xi^6)\Big]\Bigg)\Bigg\}. \end{aligned} \tag{5}$$

Here $\xi = x/a$ is a dimensionless coordinate, $\mathcal{P} = P/l$ is the contact force per unit length, while the relative contact half-width is denoted by ε, i.e.,

$$\varepsilon = \frac{a}{h}. \tag{6}$$

Note that the condition $\varepsilon \ll 1$ means that the layer thickness is assumed to be relatively large compared to the characteristic size of the contact area.

Provided the contact force P is known, formula (5) contains only one unknown contact parameter and that is the contact half-width a. The indenter displacement, which is another unknown, can be determined from the following equation [11]:

$$\begin{aligned} \mathcal{P}\Bigg\{\ln\frac{2}{\varepsilon}-d_0 \;-\; & \varepsilon^2 d_1-\frac{\varepsilon^4}{4}(d_1^2+9d_2)-\frac{\varepsilon^6}{4}(8d_1d_2+25d_3)\Bigg\}\simeq \\ \simeq\; & \frac{\pi E^* w}{2}-\frac{\pi E^* a^2}{8R}\Big(1+\varepsilon^2\frac{d_1}{2}+2\varepsilon^4 d_2+\frac{3\varepsilon^6}{32}(8d_1d_2+75d_3)\Big). \end{aligned} \tag{7}$$

At the same time, the extend of the contact zone depends on the boundary conditions for the contact pressure $q(x)$ at the end points $x = \pm a$. Namely, in the case of non-adhesive contact the contact pressure must vanish at the contact boundary, and therefore, the parameter a should satisfy the condition $q(x) = 0$.

In the case of JKR adhesive contact, the contact pressure (5) becomes singular at the contact boundary. Thus, evaluating the SIF of the contact pressure (5), which is an even function of x, we get

$$\begin{aligned} -K_{\mathrm{I}} \;\simeq\; & \frac{1}{\sqrt{\pi a}}\Bigg\{\mathcal{P}\Big(1+\varepsilon^2 d_1+\varepsilon^4\frac{9d_2}{2}+\frac{3\varepsilon^6}{4}(2d_1d_2+25d_3)\Big) \\ & -\frac{\pi E^* a^2}{4R}\Big(1+\varepsilon^4\frac{3d_2}{2}+\varepsilon^6\frac{75d_3}{8}\Big)\Bigg\}. \end{aligned} \tag{8}$$

The condition that the SIF (8) should satisfy Griffith's energy balance equation (3) implies the following equation:

$$\mathcal{P} = \frac{\pi E^* a^2}{4R}\frac{\Pi_1(\varepsilon)}{\Pi_2(\varepsilon)}-\frac{\sqrt{2\pi a E^*\Delta\gamma}}{\Pi_2(\varepsilon)}. \tag{9}$$

Here, for the sake of brevity, we have introduced the notation

$$\begin{aligned}\Pi_1(\varepsilon) &\simeq 1+\varepsilon^4\frac{3d_2}{2}+\varepsilon^6\frac{75d_3}{8},\\ \Pi_2(\varepsilon) &\simeq 1+\varepsilon^2 d_1+\varepsilon^4\frac{9d_2}{2}+\frac{3\varepsilon^6}{4}(2d_1d_2+25d_3).\end{aligned} \tag{10}$$

On the other hand, Eq. (7) can be rewritten in the form

$$w=\frac{a^2}{4R}\Theta_1(\varepsilon)+\frac{2\mathcal{P}}{\pi E^*}\Theta_2(\varepsilon), \tag{11}$$

where, in turn, we have introduced the notation

$$\begin{aligned}\Theta_1(\varepsilon) &\simeq 1+\varepsilon^2\frac{d_1}{2}+2\varepsilon^4 d_2+\frac{3\varepsilon^6}{32}(8d_1d_2+75d_3),\\ \Theta_2(\varepsilon) &\simeq \ln\frac{2}{\varepsilon}-d_0-\varepsilon^2 d_1-\frac{\varepsilon^4}{4}(d_1^2+9d_2)-\frac{\varepsilon^6}{4}(8d_1d_2+25d_3).\end{aligned} \tag{12}$$

Formulas (5), (9), and (11) provide an asymptotic solution (up to terms of order $O(\varepsilon^8)$) and constitute the fourth-order asymptotic model. At the same time, Eqs. (9), and (11) represent the force-displacement relation in a parametric form.

Observe that the asymptotic relations (5), (9), and (11) include the first four asymptotic coefficients d_0, d_1, d_2, and d_3, which are related to the kernel function by the formulas

$$d_0=\int\limits_0^\infty\frac{1-L(u)-e^{-u}}{u}du, \tag{13}$$

$$d_n=\frac{(-1)^n}{(2n)!}\int\limits_0^\infty[1-L(u)]u^{2n-1}du\quad(n=1,2,\ldots). \tag{14}$$

It is important to note that the asymptotic coefficients d_n $(n=1,2,\ldots)$ bear information about the tissue anisotropy, the degree of incompressibility, and the type of boundary conditions at the tissue/substrate interface.

In the simplest case, when the cylinder indenter is oriented longitudinally (i.e., orthogonally to the material plane of isotropy) and the frictionless contact is assumed between the tissue and the rigid substrate, we have $d_0=0.3517$, $d_1=-0.521$, $d_2=0.1349$, and $d_3=-0.0346$.

4. Asymptotic approximation for the pull-off force

Differentiating Eq. (9) with respect to a and taking into account (6), we get

$$\begin{aligned}\frac{\partial\mathcal{P}}{\partial a} \;\simeq\; & \frac{\pi E^* a}{2R}\left(\frac{\Pi_1(\varepsilon)}{\Pi_2(\varepsilon)}+\frac{\varepsilon}{2\Pi_2(\varepsilon)^2}\left[\Pi_1'(\varepsilon)\Pi_2(\varepsilon)-\Pi_2'(\varepsilon)\Pi_1(\varepsilon)\right]\right)\\ & -\sqrt{\frac{\pi E^*\Delta\gamma}{2a}}\,\frac{\left[\Pi_2(\varepsilon)-2\varepsilon\Pi_2'(\varepsilon)\right]}{\Pi_2(\varepsilon)^2}.\end{aligned} \tag{15}$$

Looking for an extremum of the function $\mathcal{P}(a)$ and equating the right-hand of Eq. (15) to zero, we arrive at the equation

$$\frac{\varepsilon\Big(\Pi_1(\varepsilon)+\varepsilon(2\Pi_2(\varepsilon))^{-1}\big[\Pi_1'(\varepsilon)\Pi_2(\varepsilon)-\Pi_2'(\varepsilon)\Pi_1(\varepsilon)\big]\Big)^{2/3}}{\big(1-2\varepsilon\Pi_2(\varepsilon)^{-1}\Pi_2'(\varepsilon)\big)^{2/3}}=\beta \tag{16}$$

with respect to the critical value, ε_c, of the ratio $\varepsilon = a/h$.

Observe that the left-hand side of Eq. 16 is dimensionless, and therefore, its right-hand side should be the same, so that the parameter

$$\beta=\left(\frac{2R^2\Delta\gamma}{\pi E^* h^3}\right)^{1/3}, \tag{17}$$

which appeared in Eq. 16, is dimensionless too.

The following formula provides an asymptotic solution to Eq. (16) with a relative accuracy of 2 percent for $\beta \le 0.15$:

$$\varepsilon_c \simeq \beta\Big(1-2d_1\beta^2+7\beta^4(d_1^2-3d_2)-\frac{11\beta^6}{6}(16d_1^3-120d_1d_2+75d_3)\Big). \tag{18}$$

The substitution of (18) into Eq. (9) yields the critical value of the line contact force

$$\mathcal{P}_c \simeq -\frac{3\pi E^* h^2}{4R}\beta^2\Big\{1-d_1\beta^2+\beta^4(3d_1^2-5d_2)-\beta^6\Big(\frac{35}{3}d_1^3-50d_1d_2+175d_3\Big)\Big\}. \tag{19}$$

In view of (2), (17), and (19), we note that in the leading order approximation for the pull-off force and the critical half-width of the contact zone are

$$P_c \sim -l\Big(\frac{27\pi}{16}E^*(\Delta\gamma)^2R\Big)^{1/3}, \quad a_c \sim \Big(\frac{2R^2\Delta\gamma}{\pi E^*}\Big)^{1/3}, \tag{20}$$

where l is the cylinder length.

We note that the pull-off force (20) coincides with the prediction of the 2D model for line adhesive contact [22].

Finally, taking into account the relations (20), we introduce dimensionless variables

$$\bar a=\Big(\frac{\pi E^*}{2R^2\Delta\gamma}\Big)^{1/3}a, \quad \bar{\mathcal{P}}=\Big(\frac{27\pi}{16}E^*(\Delta\gamma)^2R\Big)^{-1/3}\mathcal{P}, \quad \bar w=\Big(\frac{4\pi E^*}{\Delta\gamma\sqrt{R}}\Big)^{2/3}w \tag{21}$$

and express Eqs. (9), (11) in the non-dimensional form as

$$\bar{\mathcal{P}}=\frac{\bar a^2}{3}\frac{\Pi_1(\varepsilon)}{\Pi_2(\varepsilon)}-\frac{4\bar a^{1/2}}{3\Pi_2(\varepsilon)}, \tag{22}$$

$$\bar w=\bar a^2\Big(\Theta_1(\varepsilon)+2\Theta_2(\varepsilon)\frac{\Pi_1(\varepsilon)}{\Pi_2(\varepsilon)}\Big)-\frac{8\Theta_2(\varepsilon)}{\Pi_2(\varepsilon)}\bar a^{1/2}, \tag{23}$$

where $\varepsilon = \beta\bar a$ in light of (6) and (17).

In the cylindrical lateral depth-sensing indentation tests for thin adhesive elastic samples, formulas (22) and (23) can be used for the development of the BG method [23,24], which is based on iterative linearized optimization technique for a nonlinear ill-posed material parameter identification problem.

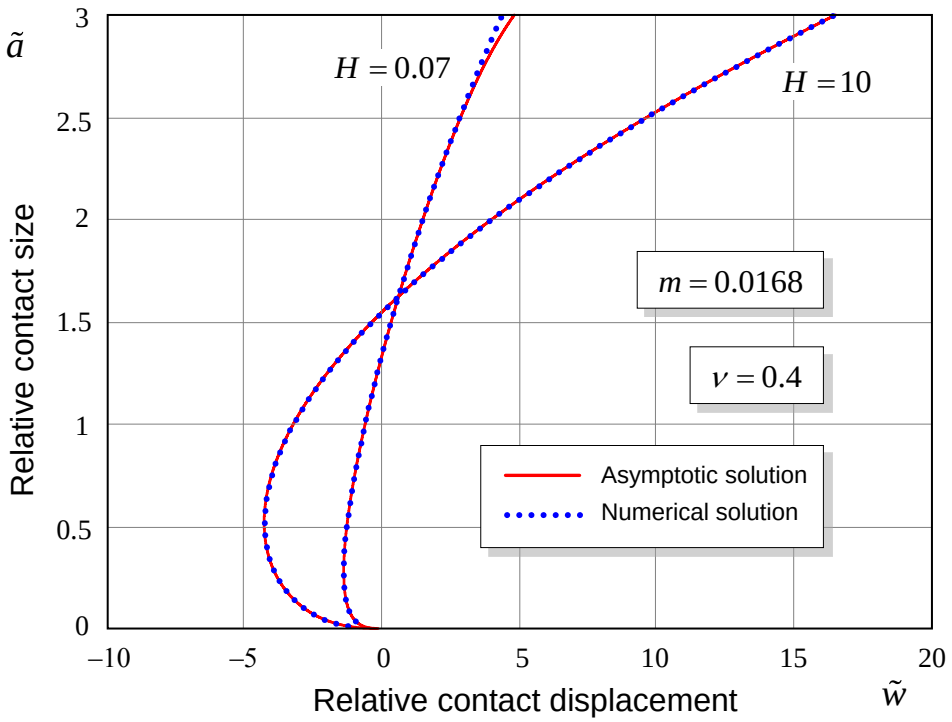

Figure 2. Variation of the contact region's non-dimensionalized size, $\tilde{a}$, with the indenter's displacement, $\tilde{w}$, for two values of the relative layer thickness $H = h/R$. Numerical solution was obtained in [20].

5. Comparison with numerical solution

Recently, Dalmeya et al. [20] investigated the 2D contact of a cylindrical punch with an isotropic adhesive elastic layer bonded to a rigid substrate in the framework of the Dugdale—Barenblatt adhesive zone model and extended their general solution to the JKR model as well. In this case the kernel function $L(u)$, which enters the governing integral equation (1), is given by the following expression [25]:

$$L(u) = \frac{2\varkappa \operatorname{sh}(2u) - 4u}{2\varkappa \operatorname{ch}(2u) + 1 + \varkappa^2 + 4u^2}.$$

Here, $\varkappa = 3 - 4\nu$ is Kolosov's elastic constant, while the effective elastic modulus E^* is related to Young's modulus, E, and Poisson's ratio, ν, by the well known formula $E^* = E/(1-\nu^2)$.

According to Dalmeya et al. [20], we make use of the following normalization [26]:

$$\tilde{a} = \Big(\frac{4E^*}{3\pi R^2 \Delta\gamma}\Big)^{1/3} a, \quad \tilde{\mathcal{P}} = \frac{\mathcal{P}}{\pi\Delta\gamma}, \quad \tilde{w} = \Big(\frac{16E^{*2}}{9\pi^2(\Delta\gamma)^2 R}\Big)^{1/3} w. \tag{24}$$

So, in view of (24), Eqs. (9) and (11) can be now rewritten in the form

$$\tilde{\mathcal{P}} = \frac{3\pi\tilde{a}^2}{16m}\frac{\Pi_1(\varepsilon)}{\Pi_2(\varepsilon)} - \sqrt{\frac{3}{2}}\frac{m^{1/6}\tilde{a}^{1/2}}{\Pi_2(\varepsilon)}, \tag{25}$$

$$\tilde{w} = \frac{\tilde{a}^2}{4}\Theta_1(\varepsilon) + \frac{8m}{3\pi}\tilde{\mathcal{P}}\Theta_2(\varepsilon), \tag{26}$$

where m is a dimensionless adhesion parameter given by

$$m = \Big(\frac{3\pi\Delta\gamma}{4E^*R}\Big)^{1/3}. \tag{27}$$

At the same time, the relative half-width of the contact zone is evaluated as

$$\varepsilon = \frac{m\tilde{a}}{H}, \quad H = \frac{h}{R}. \tag{28}$$

Fig. 2, shows a good correlation of the analytical solution (25), (26) with the results of numerical simulations [20] for a specific value of the adhesion parameter $m = 0.0168$ (which, e.g., corresponds to an adhesive elastic layer with $\Delta\gamma = 0.02$ J, $E = 0.083$ MPa, and $\nu = 0.4$, and a cylinder indenter with $R = 10$ cm). It is readily seen that the accuracy of the analytical predictions diminishes as the relative layer thickness H (see Eq. $(28)_2$) decreases.

6. Incompressibility assumption in the non-adhesive cylindrical lateral indentation

The case of incompressible material is very important for biomedical and biomechanical applications. However, since the development of the cylindrical lateral depth-sensing indentation technique with the effect of adhesion requires a special analysis, here we contribute to the understanding of the effect of incompressibility. If the tissue material is assumed to be incompressible, then the following condition must be satisfied: $\varepsilon_{11} + \varepsilon_{22} + \varepsilon_{33} = 0$. It is known that this incompressibility condition imposes two additional constrains on the components of the compliance tensor. Thus, for an incompressible transversely isotropic material only 3 material constants remain independent and the following relations hold [27,28]:

$$\nu_{\|} = \frac{1}{2}, \quad \nu = 1 - \frac{E}{2E_{\|}}. \tag{29}$$

At the same time, the condition of positive definiteness of the compliance tensor reduces to

$$E < 4E_{\|}. \tag{30}$$

Since Poisson's ratio $\nu_{\|}$ is known in advance (see the first formula (29)), while Poisson's ratio ν is expressed in terms of Young's moduli E and $2E_{\|}$ (see the second formula (29)), the problem of material parameters identification reduces to the evaluation of the following elastic constants: E, $E_{\|}$, and $G_{\|}$. However, instead of these three dimensional parameters, it is convenient to make use of the transverse Young's modulus E and two dimensionless ratios

$$n = \frac{E_{\|}}{E}, \quad k = \frac{G_{\|}}{E}. \tag{31}$$

Observe that in the compressible case [11], instead of k, it was suggested to employ the shear moduli ratio $m = G_{\|}/G = 2(1+\nu)G_{\|}/E$, which in view of (29) now depends on the parameter n.

Thus after evaluating the primary fitting elastic parameters E, n, and k, the elastic moduli and Poisson's ratios can be easily determined by formulas

$$E_{\|} = nE, \quad G_{\|} = kE, \quad \nu_{\|} = 0.5, \quad \nu = 1 - \frac{1}{2n}, \tag{32}$$

where, in light of (30), we should have $n > 1/4$.

During the depth-sensing frictionless indentation, the indenter displacement w (indentation depth) is related to the indentation load P (contact force) by a certain nonlinear relation, which is approximated by the following first-order asymptotic formula [11]:

$$w \simeq w_0 \frac{P}{P_0}\left(\ln\frac{4P_0}{P} + 1 - 2d_0 - \frac{3d_1}{2}\frac{P}{P_0}\right). \tag{33}$$

Here, w_0 is a characteristic length parameter, P_0 is a characteristic force parameter.

The characteristic length parameter w_0 is determined solely by the geometry of both the elastic sample and the rigid indenter as follows:

$$w_0 = \frac{h^2}{4R}. \tag{34}$$

Here, h is the film sample thickness, R is the radius of the indenter.

The characteristic force parameter P_0 is defined by the formula

$$P_0 = \frac{\pi E^* l h^2}{4R}, \tag{35}$$

where l is the length of the indenter. Note that P_0 depends on an elastic constant E^*, which will be defined later, since in the case of indentation testing, it is not known a priori.

In the transverse case (indenter is oriented parallel to the x_1-axis and perpendicular to the x_3-axis), the asymptotic constants $d_0^\perp$ and $d_1^\perp$ are evaluated according to equations (13) and (14), where the expression for the kernel function $L(u)$ depends on the values of the elastic constants [11].

In the case of an *incompressible* material, the asymptotic constants $d_0^\perp$ and $d_1^\perp$ are determined via dimensionless parameters $A_\perp$, $B_\perp$, and $\gamma_\perp$, which are given by

$$A_\perp = \frac{2n^2 - (4n-1)k}{k(4n-1)}, \quad B_\perp = 1, \quad \gamma_\perp = \frac{4n^2 E}{4n-1}. \tag{36}$$

In the transverse case (when the anisotropy declares itself at its utmost), the tissue material identification procedure can be outlined as follows. First, for some assumed value of k by fitting the set of experimental depth-load data with the analytical approximation (33) in view of (14), one can determine the elastic constants n and

$$E_\perp^* = \frac{4R}{\pi l h^2} P_0^\perp, \tag{37}$$

where $P_0^\perp$ is the corresponding best-fit value for P_0 in (33).

Further, having known $E_\perp^*$, n, and k, we can evaluate the dimensionless constant $A_\perp$ by the first formula (36), which afterwards allows the evaluation of the in-plane Young's modulus by the formula

$$E = \frac{E_\perp^*}{\gamma_\perp}\begin{cases} \dfrac{A_\perp + 1 + \sqrt{A_\perp^2 - 1}}{2\sqrt{A_\perp + \sqrt{A_\perp^2 - 1}}} & (A_\perp^2 > 1), \\ 1 \quad (A_\perp^2 = 1), \\ 2^{-1/2}\sqrt{1 + A_\perp} \quad (A_\perp^2 < 1), \end{cases} \tag{38}$$

where $\gamma_\perp$ is given by $(36)_2$.

Finally, the longitudinal Young's modulus and the longitudinal shear modulus are evaluated as follows:

$$E_{\|} = nE, \quad G_{\|} = kE. \tag{39}$$

Formulas (37), (38), and (39) solve the formulated above material properties identification problem. In the case of transverse indenter orientation, it is of interest to consider the situation of strong anisotropy (see, e.g., [29]), because the efficiency of the identification method decreases as n increases.

In the longitudinal case (indenter is oriented along the x_3-axis), we have $A^{||} = 1$ and $B^{||} = 1$. Still, formula (38) holds, provided $\gamma_{\perp}$ is replaced with $\gamma_{||} = 4nE/(4n-1)$, while the parameter $P_0^{||}$ is determined by fitting formula (33) with fixed asymptotic constants $d_0^{||}$ and $d_1^{||}$, because they are now independent of the tissue properties. It is to emphasize that fitting the experimental data for the force-displacement relationship allows to determine only one elastic constant $E_{||}^*$, so that formulas (39) do not work any more as the ratios n and k are unknown.

7. Discussion

In the present paper, we develop an asymptotic model, which represents an approximate analytical solution to the adhesive contact problem under consideration. In Section 5, the derived asymptotic solution was compared with the numerical solution under the same assumptions, and it is shown that (without calculation errors) the results almost coincide when $\varepsilon \ll 1$. However, in each instance the application of the developed theory for the explanation of experimentally observed phenomena should be demonstrated.

For weakly compressible materials, one can expect that the material identification procedure is sensitive to the choice of the Poisson's ratio values (for instance, their typical values are $\nu_{\|} = 0.49$ and $\nu = 0.95$ as assumed in [30] for a soft highly anisotropic tissue with $E_{\|}/E = 20.3$). At the same time, the value of $G_{\|}/E$ is needed for a robust estimation of the material parameters, while for the obtained value of the elastic moduli ratio $n = E_{\|}/E$ the following thermodynamic limitation imposed on the Poisson's ratio ν [31] should be preserved:

$$-1 < \nu < 1 - \frac{2\nu_{\|}^2}{n}. \tag{40}$$

Therefore, in the case of slight incompressibility, it is suggested first to solve the material parameters identification problem using the algorithm proposed in this paper under the assumption of the complete incompressibility, thus obtaining an upper bound for the Poisson's ratio ν. After that, utilizing the algorithm [11], one can adjust step-by-step the values of Poisson's ratios in such a way that the right-hand side inequality in (40) is preserved, while the approximation error is kept to a minimum.

It is also worth emphasizing that in the case of thin layers, when the size of the contact zone is much larger than the layer thickness, the concept of a weakly incompressible layer can be introduced [32], which takes into account the interplay between the material and geometrical parameters. The same approach can be utilized in the indentation problem under consideration. However, in the case of anisotropic material, one should take care of two small parameters, which define how the two bulk moduli describe the material behaviour when its incompressibility increases.

In the case of a relatively small contact zone with respect to the layer thickness, the fourth-order asymptotic solution (up to terms of order $O(\varepsilon^8)$) is obtained, and the pull-off force is expanded in terms of the non-dimensional measure of the work of adhesion. It should be noted that by developing the asymptotic expansion beyond all orders exploited for the analysis it is not possible to extend greatly the interval of applicability of the asymptotic model (see [11]).

On the other hand, by reducing the number of the terms retained in the asymptotic expansions, we reduce the accuracy of the analytical approximation. Therefore, it makes sense to utilize the first-order asymptotic model, provided its interval of applicability is kept as small as possible to minimize the approximation error.

8. Conclusion

Summarizing, in the present paper, the first-order asymptotic model for the frictionless unilateral contact between a rigid cylindrical indenter and a layer of elastic tissue is applied for the development of cylindrical lateral non-adhesive indentation tests for transversely isotropic samples under the assumption of tissue incompressibility. The obtained asymptotic solution of the corresponding JKR adhesive contact problem can be applied for estimating the effect of adhesion in the lateral indentation. The asymptotic model can be effectively used for small values of the dimensionless parameter β^3, which is proportional to the work of adhesion and the indenter radius squared, on the one side, and inversely proportional to the effective elastic modulus and the elastic layer thickness cubed, on the other.

9. Acknowledgment

The authors acknowledge support from the FP7 IRSES Marie Curie grant TAMER No 610547 and also thank M. Paukshto for a fruitful discussion. One of the authors (IA) is also grateful to the DAAD (German Academic Exchange Service — Deutscher Akademischer Austausch Dienst) for financial support during his stay at the TU Berlin.

References

[1] Delalleau, A., Josse, G., Lagarde, J.-M., Zahouani, H., and Bergheau, J.-M., *J. Biomech.* 39, 1603–1610 (2006).
[2] Egorov, V., Tsyuryupa, S., Kanilo, S., Kogit, M., and Sarvazyan, A., *Med. Eng. Phys.* 30, 206–212 (2008).
[3] Geerligs, M., van Breemen, L., Peters, G., Ackermans, P., Baaijens, F., and Oomens, C., *J. Biomech.* 44, 1176–1181 (2011).
[4] Pailler-Mattei, C., Bec, S., and Zahouani, H., *Med. Eng. Phys.* 30, 599–606 (2008).
[5] Flynn, C., Taberner, A., and Nielsen, P., *Med. Eng. Phys.* 33, 610–619 (2011).
[6] Annaidh, A.N., Bruyére, K., Destrade, M., Gilchrist, M.D., and Otténio, M., *J. Mech. Behav. Biomed. Mater.* 5, 139–148 (2012).
[7] Lin, D.C., and Horkay, F., *Soft Matter* 4, 669–682 (2008).
[8] Humphrey, J.D., *Proc. Roy. Soc. Lond. A* 459, 3–46 (2003).
[9] Pailler-Mattei, C., and Zahouani, H., *Tribol. Int.* 39, 12–21 (2006).
[10] Harrison, S.M., Bush, M.B., and Petros, P.E., *Med. Eng. Phys.* 29, 307–315 (2007).
[11] Argatov, I.I., Mishuris, G.S., and Paukshto, M.V., *Eur. J. Mech. A/Solids* 49, 299–307 (2015).
[12] Aleksandrov, V.M., *J. Appl. Math. Mech.* 70, 128–138 (2006).
[13] Erbaş, B., Yusufoğlu, E., and Kaplunov, J., *J. Eng. Math.* 70, 399–409 (2011).
[14] Choi, A.P.C., and Zheng, Y.P., *Med. Biol. Eng. Comput.* 43, 258–264 (2005).
[15] Johnson, K.L., Kendall, K., and Roberts, A.D., *Proc. R. Soc. London, Ser. A* 324, 301–313 (1971).
[16] Borodich, F.M., *Adv. Appl. Mech.* 47, 225–366 (2014).
[17] Chen, S., Yan, C., and Soh, A., *Int. J. Solids Struct.* 45, 676–687 (2008).
[18] Guo, X., and Jin, F., *Int. J. Solids Struct.* 46, 3607–3619 (2009).
[19] Borodich, F.M., Galanov, B.A., Keer, L.M., and Suarez-Alvarez, M.M., *Mech. Mater.* 75, 34–44 (2014).
[20] Dalmeya, R., Sharma, I., and Upadhyay, C., *J. Adhesion* 88, 1–31 (2012).
[21] Maugis, D., *Langmuir* 11, 679–682 (1995).
[22] Chaudhury, M.K., Weaver, T., Hui, C.Y., and Kramer, E.J., *J. Appl. Phys.* 80, 30–37 (1996).

[23] Borodich, F.M., and Galanov, B.A., *Proc. Roy. Soc. A* 464, 2759–2776 (2008).
[24] Borodich, F.M., Galanov, B.A., Gorb, S.N., Prostov, M.Y., Prostov, Y.I., and Suarez-Alvarez, M.M., *Macromol. React. Eng.* 7, 555–563 (2013).
[25] Vorovich, I.I., Aleksandrov, V.M., and Babeshko, V.A., Non-classical Mixed Problems of the Theory of Elasticity, (Nauka, Moscow, 1974).
[26] Maugis, D., *J. Colloid Interface Sci.* 150, 243–269 (1992).
[27] Garcia, J.J., Altiero, N.J., and Haut, R.C., *J. Biomech. Eng.* 120, 608–613 (1998).
[28] Itskov, M., and Aksel, N., *Acta. Mech.* 157, 81–96 (2002).
[29] Andrianov, I.V., and Starushenko, G.A., *Technische Mechanik* 28, 121–125 (2008).
[30] Gilchrist, M.D., Murphy, J.G., Parnell, W., and Pierrat, B., *Int. J. Solids Struct.* 51, 3857–3865 (2014).
[31] Lempiere, B.M., *AIAA J. Tech. Notes* 6, 2226–2227 (1968).
[32] Mishuris, G., *Arch. Mech.* 56, 103–115 (2004).